AGU PUBLICATIONS

Geophysical Research Letters

RESEARCH LETTER

10.1002/2016GL068550

Key Points:
- Peat and organic-rich soil will insulate permafrost from emerging environmental conditions
- ALT formation is weakly dependent to the amount of water on the landscape, but in combination with snow depth can trigger talik formation
- Snow depth will increase ALT and is codependant on inundation depth and peat thickness

Supporting Information:
- Supporting Information S1

Correspondence to:
A. L. Atchley,
aatchley@lanl.gov

Citation:
Atchley, A. L., E. T. Coon, S. L. Painter, D. R. Harp, and C. J. Wilson (2016), Influences and interactions of inundation, peat, and snow on active layer thickness, *Geophys. Res. Lett.*, *43*, doi:10.1002/2016GL068550.

Received 8 MAR 2016
Accepted 1 MAY 2016
Accepted article online 4 MAY 2016

Published 2016. This article is a US Government work and is in the public domain in the United States of America.

Influences and interactions of inundation, peat, and snow on active layer thickness

Adam L. Atchley[1], Ethan T. Coon[1], Scott L. Painter[2], Dylan R. Harp[1], and Cathy J. Wilson[1]

[1]Los Alamos National Laboratory, Los Alamos, New Mexico, USA, [2]Climate Change Science Institute and Environmental Sciences Division, Oak Ridge National Laboratory, Oak Ridge, Tennessee, USA

Abstract Active layer thickness (ALT), the uppermost layer of soil that thaws on an annual basis, is a direct control on the amount of organic carbon potentially available for decomposition and release to the atmosphere as carbon-rich Arctic permafrost soils thaw in a warming climate. We investigate how key site characteristics affect ALT using an integrated surface/subsurface permafrost thermal hydrology model. ALT is most sensitive to organic layer thickness followed by snow depth but is relatively insensitive to the amount of water on the landscape with other conditions held fixed. The weak ALT sensitivity to subsurface saturation suggests that changes in Arctic landscape hydrology may only have a minor effect on future ALT. However, surface inundation amplifies the sensitivities to the other parameters and under large snowpacks can trigger the formation of near-surface taliks.

1. Introduction

The upper 3 m of soil in Arctic permafrost regions contains an estimated 1030 Pg of organic carbon [*Hugelius et al.*, 2014; *Tarnocai et al.*, 2009], which is significantly more carbon than currently in the atmosphere [*Houghton*, 2007]. As Arctic air and permafrost temperatures increase [*Oelke et al.*, 2004; *Osterkamp*, 2005], vast stores of organic carbon are vulnerable to thawing, decomposition, and release to the atmosphere as greenhouse gases [*Davidson and Janssens*, 2006; *Schuur et al.*, 2008], potentially accelerating climate change. The amount of carbon that is available for decomposition in Arctic soils is directly related to the active layer thickness (ALT), the thickness of the soil layer that thaws each year. For that reason, considerable attention has been focused on projecting ALT in future climates [e.g., *Koven et al.*, 2013; *Slater and Lawrence*, 2013].

Freezing and thawing in soils is a highly nonlinear process that strongly couples hydrologic and thermal processes through the latent heat of phase change, cryosuction, advective heat transport, thermal conductivity dependence on frozen and unfrozen moisture content, and hydraulic conductivity dependence on ice content [e.g., *Painter*, 2011]. In addition, ALT further depends on surface processes and properties, such as the surface energy balance and the environmental conditions of snow depth, surface water, and surface albedo. These processes are nonlinear, strongly coupled, and many are competing. This complex nature of coupled but competing processes has resulted in an incomplete understanding of how ALT varies with local environmental conditions. In this Letter we use a recently developed permafrost simulation tool to untangle process sensitivity of ALT to key environmental controls: thickness of the tundra organic layer, snowdepth, and amount of water on the landscape. We focus on this subset of environmental controls because they affect competing processes, which leads to a more complicated and less understood relationship to ALT compared to other environmental controls.

Organic-rich soil regulates thermal conduction and transfer of surface energy to the permafrost [*Beringer et al.*, 2001; *Hinzman et al.*, 1991; *Nicolsky et al.*, 2007], as is well established in the modeling community [*Chadburn et al.*, 2015a; *Dankers et al.*, 2011; *Lawrence and Slater*, 2008; *O'Donnell et al.*, 2009; *Rinke et al.*, 2008]. However, liquid and gas saturations also play a role in determining soil thermal conductivity [*Johansen*, 1975], which link saturated soils to deeper ALT [*Gamon et al.*, 2012; *Wainwright et al.*, 2015; *Zona et al.*, 2011]. Ponded water and surface saturation further affect the surface energy balance by regulating surface albedo and energy partitioning to latent heat fluxes [*Liljedahl et al.*, 2011]. Surface water is controlled by microtopography and macrotopography [*Engstrom et al.*, 2005; *Muster et al.*, 2012]. Soil moisture is influenced by subsurface flow [*Helbig et al.*, 2013; *McKenzie and Voss*, 2013; *Rowland et al.*, 2011; *Yi et al.*, 2014] along with peat, and partially decomposed organic matter, which tend to have high residual saturations and soil moisture holding capacities [*Letts et al.*, 2000]. Snowmelt also supplies water to soil, Arctic ponds, and low-elevation topography [*Rovansek et al.*, 1996; *Woo et al.*, 2006], seasonally affecting soil moisture.

Bulk thermal conductivity of peat is highly dependent on the saturation state and increases with decreased gas saturation [*Andersland and Anderson*, 1978; *Farouki*, 1981]. It is speculated that high porosities of organic soil [*Letts et al*., 2000; *Yi et al*., 2009] allow for broad ranges of peat thermal conductivity and latent heat demands due to large changes in volumetric water content [*O'Donnell et al*., 2009]. However, both mineral and organic soils can have porosities above 50% in polygonal tundra [*Hinzman et al*., 1991; *Nicolsky et al*., 2009] due to frost mechanics; therefore, the entire soil profile maybe subject to large thermal property variation from transient hydrological conditions.

The low thermal conductivity of snow moderates atmospheric winter conditions and prevents soils from experiencing large temperature swings, which results in warmer winter surface soil temperatures [*Hinkel and Hurd*, 2006; *Zhang*, 2005]. For example, horizontally varying snow depth by 30 cm due to microtopography resulted in up to 10°C soil temperature changes [e.g., *Sturm and Holmgren*, 1994]. However, given that ALT is measured in late summer when snow is not present, it is uncertain how much the winter influence of snow will affect ALT [*Chadburn et al*., 2015b].

Thus, snow depth, organic layer thickness, and the amount of water in the landscape influences individual thermal hydrological processes in ways that are either known empirically or can be deduced from basic physical understanding. However, it is the interacting effects of these processes that control active layer dynamics, and to understand ALT, it is necessary to turn to numerical simulation.

2. Methods

Process-rich models of thermal hydrological dynamics can help untangle the physical controls of thermal hydrological phenomena [*Endrizzi et al*., 2014; *Painter*, 2011; *Westermann et al*., 2016], especially when models have been systematically refined using measured data [*Nicolsky et al*., 2007; *Rawlins et al*., 2013; *Schaefer et al*., 2009]. Here an ensemble of 1D thermal hydrology simulations are generated using the Advanced Terrestrial Simulator (ATS), which has been extensively refined in an iterative observation-model framework to reduce model structure error [*Atchley et al*., 2015a], to systematically sample environmental conditions such that each realization represents specific environmental conditions encountered in tundra. ALT sensitivities are calculated as slope coefficients from linear regressions along 1D transects through the ensemble of varied environmental conditions. Color maps of these sensitivities expose the interactive influences between the environmental conditions and ALT.

2.1. Model Description

ATS is a collection of process models and physics-based model couplers within the Amanzi-ATS modeling framework [*Moulton et al*., 2011]. A process management tool called Arcos [*Coon et al*., 2016] is used to manage the significant degree of model complexity arising from these integrated surface/subsurface thermal hydrology models. ATS implements the modeling strategy for permafrost systems outlined by *Painter et al*. [2013]. Energy and water fluxes from a snow and surface energy balance model [*Atchley et al*., 2015a] are coupled to potentially frozen surface water, which is then coupled to a variably saturated subsurface domain. Mass and energy conservation equations are described by *Painter* [2011], *Frampton et al*. [2011], and *Karra et al*. [2014], using the explicit "freezing point depression" model of *Painter and Karra* [2014] to partition ice and liquid phases in unsaturated conditions. This model allows liquid to coexist with ice below 0°C and flow due to cryosuction. The internal energy of the soil water system is a volumetric average of the internal energies of the components vapor, liquid, ice, and soil solids. Latent heat is represented implicitly through the differences in internal energies of vapor, liquid, and ice. Bulk thermal conductivity is related to porosity and liquid, ice, and gas saturations following the methods of *Johansen* [1975] and *Peters-Lidard et al.* [1998]. Snow depth is temporally variable because of snowfall, snowmelt, sublimation, and aging. The snow model is described in *Atchley et al*. [2015a] and Text S1 in the supporting information.

2.2. Model Configuration

We consider an ensemble of one-dimensional columns and interpret each as a large-scale representation of a hypothetical Arctic watershed, consistent with contemporary conceptualizations in the land surface components of Earth systems models [e.g., *Clark et al*., 2015]. Each realization prescribes environmental conditions for a 1-D column model with a 2 cm moss layer at the surface followed by a specified peat layer thickness and a mineral layer that extends to a depth of 50 m. The moss is discretized at 1 cm, below which cell

discretization is 2 cm; therefore, the ALT is resolved to plus or minus 2 cm. Thermal hydrologic parameters for moss, peat, and mineral soil layers are listed in Table S1 in the supporting informaiton [*Atchley et al*., 2015b]. ALT uncertainty caused by subsurface parameter uncertainty is detailed by *Harp et al*. [2015] and found to be less than climate uncertainty. Meteorological data from Barrow, AK, is used for the surface energy balance (Text S2).

We scanned peat thickness from 2 to 40 cm and snowfall amount from 0 to 3 times the normal precipitation amount, which corresponded to an approximate snow depth range of 0 to 1.2 m. In addition, we varied the amount of water in the landscape, which is controlled in reality by precipitation, evapotranspiration, and runoff. Specifically, we impose a "fill and spill" condition and varied the spill-point elevation. That is, the water table was dynamically calculated but was limited to a specified maximum value established by assigning atmospheric pressure at the maximum water table elevation (spill-point elevation). All subsurface cells above the spill-point were assigned a seepage boundary condition that allowed excess water to flow out of the column laterally. By scanning this spill-point elevation from −51 cm below the soil surface to 31 cm above the soil surface we thus tune between well drained to poorly drained landscapes. The mean liquid saturation is a model outcome controlled by the spill-point elevation; given the range of spill-points prescribed, mean liquid saturation of the unfrozen portion of the column varied from 59% to 100% (Figures S1 and S2 and Text S3). Fourteen different snowfall depths, 27 subsurface, and 30 surface spill-point elevations and 20 peat thicknesses are tested for a total of 15,960 realizations.

2.3. Model Spin-Up and Simulation

Each model run involved three steps: a two-step initialization, followed by a 4 year simulation. First, a deep permafrost initial condition for all combinations of peat thickness and spill-point elevations was established by freezing from below with a −9.5°C bottom temperature. It is important to set the spill-point and peat thickness before freezing the column so that as ice forms and pore volume is taken up by the volume expansion of the liquid-to-ice phase change; water can seep out above the designated spill-point elevation. As a result, various liquid and ice saturations were spun-up consistent with the specified environmental conditions. Realizations with a spill-point above the soil surface were initialized with a fully saturated column, where snow height and surface runoff evolved as a result of meteorological conditions. In the second part of the spin-up process, a cyclical thermal steady state, defined as less than 0.1 mm change in ALT, was achieved from a 10 year spin-up using average decadal meteorological data from 1 October 1998 to 30 September 2009 at Barrow, AK. As the thaw depth increases and snowmelt and precipitation infiltrates, water may seep out of the subsurface to the point of the assigned spill-point or replenish water lost from evaporation (Figure S2 and Text S3). Finally, we ran all realizations forward 4 years (Text S2) specifying all three environmental variables (peat thickness, spill-point elevation, and snowfall amount). We determined ALT for each realization as the deepest thaw point during the fourth year.

3. Results

The simulated ALT ranged from a low of 24 cm to a high of 56 cm, which is within the range observed at Barrow, Alaska [*Cable and Romanovsky*, 2014; *Sloan et al*., 2014]. ALT has a strong negative correlation to peat thickness (Table 1), as the largest ALT was simulated when peat thickness is shallow (Figure 1). However, when peat thickness is greater than ALT, approximately 30 cm for conditions simulated here, the strong negative relationship ceases to exist. ALT is positively correlated to snowfall, and weakly yet positively correlation to spill-point elevation and unfrozen liquid saturation (Table 1). The transition to inundated conditions resulted in a slight increase in correlation between ALT and spill-point elevation and a stronger positive correlation between ALT and snowpack depth.

Interactions among the three environmental conditions are examined by first computing primary sensitivities along 1-D transects through the ensemble as the slope from linear regressions of ALT and single environmental conditions. The range of ALT is the primary sensitivity multiplied by the range of the sampled environmental condition (method depicted in Figure S3). Matrices of these 1-D sensitivity transects are then assembled for each environmental condition for all combinations of the other two environmental conditions. Separate sensitivity maps (Figure 2) are generated for exposed and inundated soil surface.

Table 1. Pearson's Correlation Coefficients for ALT and Each Environmental Condition

	Pearson's Correlation Coefficients		
Environmental Variable	Combined	Spill-Point Below	Spill-Point Above
Peat thickness	−0.81	−0.84	−0.80
Snowfall amount	0.44	0.41	0.47
Spill-point	0.14	0.13	0.15
Unfrozen liquid saturation	0.13	0.16	--

Increasing peat thickness from 2 to 40 cm causes the ALT to decrease because peat is a better thermal insulator than mineral soil. The magnitude of that decrease ranged from 12 to 25 cm, depending on the values of the other two environmental conditions (Figures 2a and 2b). Snow and spill-point elevation interact with peat thickness to control ALT when the soil surface is exposed, but only snow interacts with peat thicknesses when the soil surface is inundated.

The sensitivity of ALT to spill-point elevation is modest, regardless of whether the soil surface is exposed or inundated (Figures 2c and 2d and Table 1). Specifically, changing the spill-point elevation from −51 to 0 changes the ALT by an insignificant amount except when the peat thickness is small, in which case the change is at most 8 cm (Figure 2c). When the landscape is inundated (Figure 2d) ALT sensitivity to the spill-point strengthens, but is still low unless the snow multiplier is large.

Changing the snowfall from 0 to 3 times the base snowfall resulted in an ALT change between 4 and 18 cm (Figures 2e and 2f), with the largest ALT sensitivity to snowfall occurring in inundated conditions. It is important to note that large snowpacks and deeply inundated landscape led to the formation of a surface talik, which did not reach a cyclic steady state within the 4 year simulation. Thus, at snowfall multipliers approximately greater than 2.2 and spill-point elevations approximately greater than 27 cm, the sensitivity coefficients refer to maximum annual talik depth.

4. Discussion

4.1. Peat Thickness

The strong negative dependence of ALT on peat thickness is due to the differences in thermal properties of peat versus mineral soil. First, peat is less thermally conductive than mineral soil for all saturations states, especially during winter when the subsurface is frozen and ice content is high (Figure 3). Second, the amount of energy needed to melt ice, the latent heat of fusion, is approximately one and half times greater in peat than mineral soils (Table S2), due to the high porosity and residual saturation of peat. Therefore, peat both insulates permafrost during the summer, as has been shown empirically [*Shur and Jorgenson*, 2007; *Yi et al.*, 2007] and by simulation [*Lawrence and Slater*, 2008; *Schaefer et al.*, 2009], and requires more energy to thaw due to greater latent heat of fusion demands. The higher thermal conductivity for mineral soil at all ice/liquid/gas saturation states (Figure 3) and the small amount of energy needed to thaw mineral soil results in deeper ALT when peat is thin (Figure 1).

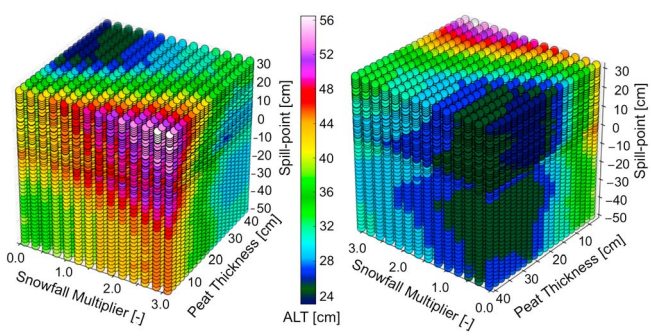

Figure 1. Full ensemble ALT results with snowfall multiplier range from 0 to 3, peat thickness from 2 to 40 cm, and a spill-point elevation range from −0.51 m below the soil surface to 0.31 m above the soil surface. The right cube is the reverse perspective of the left cube.

4.2. Inundation State

The modest ALT sensitivity to spill-point below the surface is a result of two competing effects as the subsurface becomes saturated. First, thermal conductivity increases for both peat and mineral soil as liquid and ice saturation increases (Figure 3), which results in more energy flowing into the subsurface. However, increased ice saturation

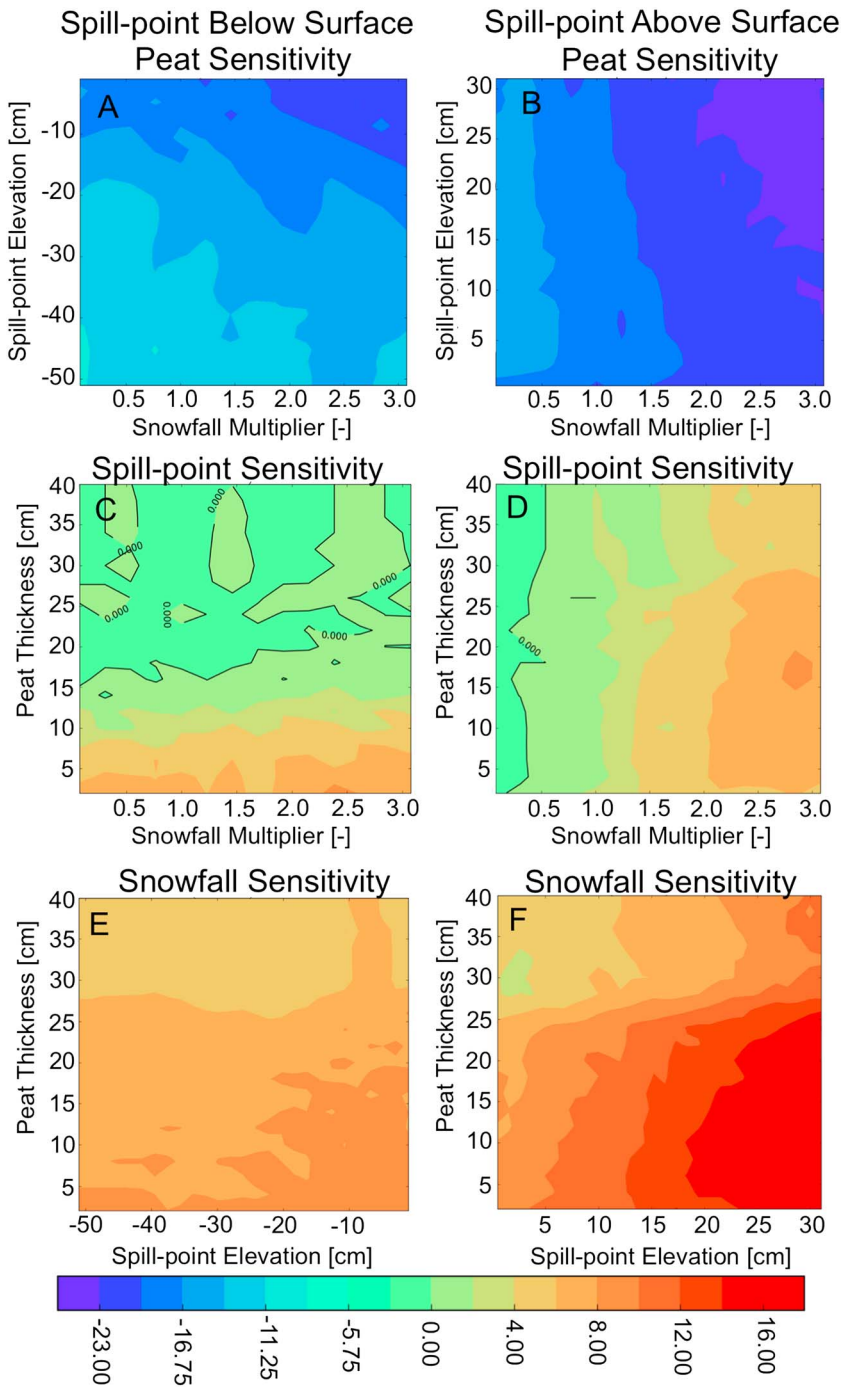

Figure 2. Sensitivities of the ALT to (a and b) peat thickness, (c and d) spill-point elevation, and (e and f) snow depth for exposed (Figures 2a, 2c, and 2e) and inundated (Figures 2b, 2d, and 2f) soil surface conditions. The slope of the change in ALT is multiplied by the range of change in environmental condition and plotted in units of ALT change (cm).

also requires more energy to melt a larger mass of ice whereby the latent heat of fusion effects can cancel increases in thermal conductivity. Given that peat has large pore space, high residual saturation and a small change in thermal conductivity relative to mineral soil (Figure 3), the increased consumption of energy by latent heat of fusion in saturated peat soils can offset gains from increased thermal conductivity, resulting in ALT being insensitive to spill-point elevation changes. Conversely, if the soil is largely mineral soil, the gains in thermal conductivity outweigh the increased energy demand to melt ice, and as the soil saturates ALT will increase (Figure 2c).

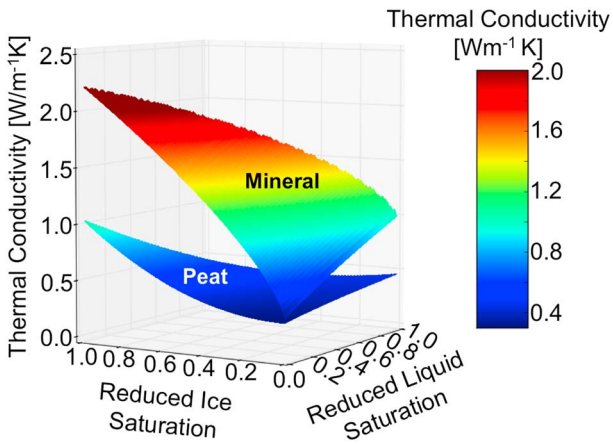

Figure 3. Thermal conductivity of mineral and peat soil for varying liquid and ice saturation. The reduced saturation reflects the residual saturation where 0.18 and 0.3 for mineral and peat, respectively, are lowest saturation endpoint for ice and liquid, plotted as 0 on both axes.

ALT sensitivity to ponded depth (spill-point above soil surface) is weak and governed by snow thickness (Figure 2d). With little to no snow present, increasing the ponded depth, and therefore winter ice mass, results in a negative ALT sensitivity due to the increased energy needed to melt more ice. However, at approximately half the normal snowpack or greater, the ALT sensitivity to spill-point elevation becomes positive. The addition of snow slows the loss of heat from surface water to the atmosphere during the fall freeze, which has the effect to extend the freeze curtain, especially for heavily inundated areas that have a larger mass of water undergoing freezing. As ponded water and snow depth increases, a threshold can be crossed where the near surface does not fully freeze during the winter resulting in a talik (demonstrated in Figure 4b, for the large snowfall amount).

4.3. Snow Depth

Snow depth had the greatest effect on soil temperature during the winter (Figure 4), with more pronounced winter insulation in the inundated cases, because a conductive layer of ice exists below the snow. Much of the soil temperature differences between realizations with different snowfall amounts disappeared during the spring because energy from warm spring temperatures also conducted through small snowpacks. However, soils that have been exposed to increased winter thermal loss due to the absence of snow are colder in the deeper subsurface and require more energy inputs to thaw the soil. The increased sensitivity to snow depth for saturated columns is due to the increased thermal conductivity of water and ice that are either in direct contact with the atmosphere or are insulated by snow. The insulation resulting from snow on a saturated surface also extends the freeze curtain, where thermal loss is absorbed in latent heat of fusion (Figure 4b), which prohibits extremely low winter soil temperatures and therefore warmer summer soil temperatures and a deeper ALT (Figure 4b, inset).

5. Conclusions

ALT is most sensitive to organic layer thickness, which prevents deep thawing due to the combined affects of thermal insulation and increased latent heat effects compared to mineral soil. The strong sensitivity to peat thickness demonstrates the need for accurate characterization of peat thickness along with rates of peat

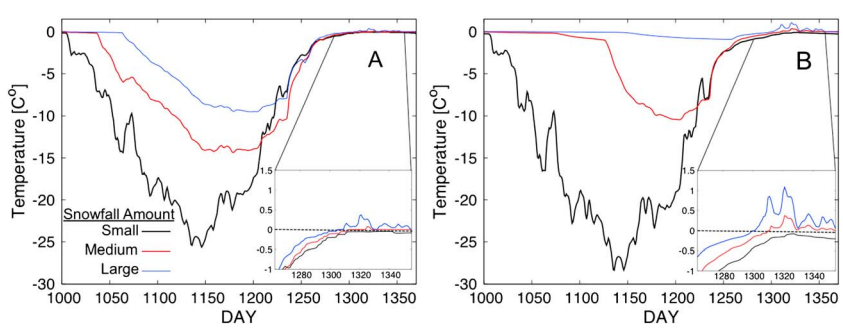

Figure 4. (a and b) Time series of 35 cm deep soil temperatures for three snowfall multipliers. "Small," "medium," and "large" correspond to 0.077, 1.46, and 3.1 snowfall multipliers, respectively. The inset magnifies the portion of the time series when ALT is determined. The peat thickness is 14 cm, and the spill-point is set at 50 cm below the surface in Figure 4a, and a spill-point of 25 cm above the surface is set in Figure 4b.

accumulation and decomposition if reliable projections of ALT are to be made in future climates. The amount of water on the landscape (drainage efficiency) showed a surprisingly modest effect on ALT, as the role of landscape inundation, both above and below the land surface, is controlled by the competing effects of increased thermal conduction and latent heat demands. Viewed in isolation, this simulation result suggests that wetting or drying of the Arctic landscape stemming from ice-wedge degradation [*Liljedahl et al*., 2016] or altered precipitation and evaporative conditions may have only a minor impact on active layer evolution. However, inundation state has a regulating effect on the remaining environmental conditions and can amplify ALT sensitivities to organic layer thickness and snow. In particular, sensitivity to snow depth is increased when the surface is inundated and as both ponded depth and snowfall increase, a threshold can be crossed where the near subsurface does not freeze during the winter, forming a talik. The combined results demonstrate the importance of considering coupled environmental conditions when projecting ALT and provide motivation for additional process representation in models that are backed by experimental and field observation to improve ALT prediction under changing conditions.

Acknowledgments
This work was supported by the Los Alamos National Laboratory, Laboratory Direction Research and Development project LDRD201200068DR and by the Next Generation Ecosystem Experiment (NGEE-Arctic) project. NGEE-Arctic is supported by the Office of Biological and Environmental Research in the DOE Office of Science. Model input files and result can be accessed at 10.5440/1240734. In addition, we wish to extend our thanks to GRL Editor Julienne Stroeve and two anonymous reviewers and who provided thoughtful commentary resulting in a quality manuscript.

References

Andersland, O., and D. Anderson (1978), *Geotechnical Engineering for Cold Regions*, McGraw-Hill, New York.

Atchley, A., S. Painter, D. Harp, E. Coon, C. Wilson, A. Liljedahl, and V. Romanovsky (2015a), Using field observations to inform thermal hydrology models of permafrost dynamics with ATS (v0.83), *Geosci. Model Dev.*, *8*, 2701–2722, doi:10.5194/gmd-8-2701-2015.

Atchley, A., S. Painter, D. Harp, E. Coon, C. Wilson, A. Liljedahl, and V. Romanovsky (2015b), Calibrated hydrothermal parameters, Barrow, Alaska, 2013, Next Generation Ecosystem Experiments Arctic Data Collection, Oak Ridge National Laboratory, Oak Ridge, Tenn.

Beringer, J., A. H. Lynch, F. S. Chapin III, M. Mack, and G. B. Bonan (2001), The representation of arctic soils in the land surface model: The importance of mosses, *J. Clim.*, *14*(15), 3324–3335, doi:10.1175/1520-0442(2001)014%3C3324:TROASl%3E2.0.CO;2.

Cable, W., and V. Romanovsky (2014), Subsurface temperature, moisture, thermal conductivity and heat flux, Barrow, Area A, B, C, D*Rep*., Next Generation Ecosystems Experiment-Arctic, Oak Ridge National Laboratory (ORNL), Oak Ridge, Tenn, doi:10.5440/1126515

Chadburn, S., E. Burke, R. Essery, J. Boike, M. Langer, M. Heikenfeld, P. Cox, and P. Friedlingstein (2015a), An improved representation of physical permafrost dynamics in the JULES land-surface model, *Geosci. Model Dev.*, *8*(5), 1493–1508, doi:10.5194/gmd-8-1493-2015.

Chadburn, S., E. Burke, R. Essery, J. Boike, M. Langer, M. Heikenfeld, P. Cox, and P. Friedlingstein (2015b), Impact of model developments on present and future simulations of permafrost in a global land-surface model, *Cryosphere*, *9*(4), 1505–1521, doi:10.5194/tc-9-1505-2015.

Clark, M. P., et al. (2015), Improving the representation of hydrologic processes in Earth System Models, *Water Resour. Res.*, *51*, 5929–5956, doi:10.1002/2015WR017096.

Coon, E. T., J. D. Moulton, and S. L. Painter (2016), Managing complexity in simulations of land surface and near-surface processes, *Environ. Modell. Software*, *78*, 134–149, doi:10.1016/j.envsoft.2015.12.017.

Dankers, R., E. Burke, and J. Price (2011), Simulation of permafrost and seasonal thaw depth in the JULES land surface scheme, *Cryosphere*, *5*(3), 773–790, doi:10.5194/tc-5-773-2011.

Davidson, E. A., and I. A. Janssens (2006), Temperature sensitivity of soil carbon decomposition and feedbacks to climate change, *Nature*, *440*(7081), 165–173, doi:10.1038/nature04514.

Endrizzi, S., S. Gruber, M. Dall'Amico, and R. Rigon (2014), GEOtop 2.0: Simulating the combined energy and water balance at and below the land surface accounting for soil freezing, snow cover and terrain effects, *Geosci. Model Dev.*, *7*, 2831–2857, doi:10.5194/gmd-7-2831-2014.

Engstrom, R., A. Hope, H. Kwon, D. Stow, and D. Zamolodchikov (2005), Spatial distribution of near surface soil moisture and its relationship to microtopography in the Alaskan Arctic Coastal Plain, *Nord. Hydrol.*, *36*, 219–234.

Farouki, O. T. (1981), Thermal properties of soils, *Rep*, DTIC Document.

Frampton, A., S. Painter, S. W. Lyon, and G. Destouni (2011), Non-isothermal, three-phase simulations of near-surface flows in a model permafrost system under seasonal variability and climate change, *J. Hydrol.*, *403*(3), 352–359, doi:10.1016/j.jhydrol.2011.04.010.

Gamon, J. A., G. P. Kershaw, S. Williamson, and D. S. Hik (2012), Microtopographic patterns in an arctic baydjarakh field: Do fine-grain patterns enforce landscape stability?, *Environ. Res. Lett.*, *7*(1), 015502, doi:10.1088/1748-9326/7/1/015502.

Harp, D., A. L. Atchley, S. L. Painter, E. Coon, C. Wilson, V. Romanovsky, and J. Rowland (2015), Effect of soil property uncertainties on permafrost thaw projections: A calibration-constrained analysis, *Cryosphere*, *10*(3), 1–18, doi:10.5194/tc-10-1-2016.

Helbig, M., J. Boike, M. Langer, P. Schreiber, B. R. Runkle, and L. Kutzbach (2013), Spatial and seasonal variability of polygonal tundra water balance: Lena River Delta, northern Siberia (Russia), *Hydrogeol. J.*, *21*(1), 133–147, doi:10.1007/s10040-012-0933-4.

Hinkel, K. M., and J. K. Hurd Jr. (2006), Permafrost destabilization and thermokarst following snow fence installation, Barrow, Alaska, USA, *Arct. Antarct. Alp. Res.*, *38*(4), 530–539, doi:10.1657/1523-0430(2006)38%5B530:PDATFS%5D2.0.CO;2.

Hinzman, L., D. Kane, R. Gieck, and K. Everett (1991), Hydrologic and thermal properties of the active layer in the Alaskan Arctic, *Cold Reg. Sci. Technol.*, *19*(2), 95–110, doi:10.1016/0165-232X(91)90001-W.

Houghton, R. (2007), Balancing the global carbon budget, *Annu. Rev. Earth Planet. Sci.*, *35*, 313–347, doi:10.1146/annurev.earth.35.031306.140057.

Hugelius, G., J. Strauss, S. Zubrzycki, J. W. Harden, E. Schuur, C.-L. Ping, L. Schirrmeister, G. Grosse, G. J. Michaelson, and C. D. Koven (2014), Estimated stocks of circumpolar permafrost carbon with quantified uncertainty ranges and identified data gaps, *Biogeosciences*, *11*(23), 6573–6593, doi:10.5194/bg-11-6573-2014.

Johansen, O. (1975), Thermal conductivity of soils, PhD thesis, Univ. of Trondheim, Trondheim, Høgskoleringen 1, 7034 Trondheim, Norway.

Karra, S., S. Painter, and P. Lichtner (2014), Three-phase numerical model for subsurface hydrology in permafrost-affected regions (PFLOTRAN-ICE v1. 0), *Cryosphere*, *8*(5), 1935–1950, doi:10.5194/tc-8-1935-2014.

Koven, C. D., W. J. Riley, and A. Stern (2013), Analysis of permafrost thermal dynamics and response to climate change in the CMIP5 Earth System Models, *J. Clim.*, *26*(6), 1877–1900, doi:10.1175/JCLI-D-12-00228.1.

Lawrence, D. M., and A. G. Slater (2008), Incorporating organic soil into a global climate model, *Clim. Dyn.*, *30*(2–3), 145–160, doi:10.1007/s00382-007-0278-1.

Letts, M. G., N. T. Roulet, N. T. Comer, M. R. Skarupa, and D. L. Verseghy (2000), Parametrization of peatland hydraulic properties for the Canadian Land Surface Scheme, *Atmos.-Ocean*, *38*(1), 141–160, doi:10.1080/07055900.2000.9649643.

Liljedahl, A. K., J. Boike, R. P. Daanen, A. N. Fedorov, G. V. Frost, G. Grosse, L. D. Hinzman, Y. Iijma, J. C. Jorgenson, and N. Matveyeva (2016), Pan-Arctic ice-wedge degradation in warming permafrost and its influence on tundra hydrology, *Nat. Geosci.*, *9*, 312–318, doi:10.1038/ngeo2674.

Liljedahl, A., L. Hinzman, Y. Harazono, D. Zona, C. Tweedie, R. D. Hollister, R. Engstrom, and W. Oechel (2011), Nonlinear controls on evapotranspiration in arctic coastal wetlands, *Biogeosciences*, *8*(11), 3375–3389, doi:10.5194/bg-8-3375-2011.

McKenzie, J. M., and C. I. Voss (2013), Permafrost thaw in a nested groundwater-flow system, *Hydrogeol. J.*, *21*(1), 299–316, doi:10.1007/s10040-012-0942-3.

Moulton, D., M. Berndt, M. Buskas, R. Garimella, L. Prichett-Sheats, G. Hammond, M. Day, and J. Meza (2011), High-level design of Amanzi, the multi-process high performance computing simulator, *Rep.*, ASCEM-HPC-2011-03-1, U.S. Department of Energy, Washington, D. C. [Available at http://esd1.lbl.gov/files/research/projects/ascem/thrusts/hpc/ASCEM-HPC-HighLevelDesign_2011-final.pdf.]

Muster, S., M. Langer, B. Heim, S. Westermann, and J. Boike (2012), Subpixel heterogeneity of ice-wedge polygonal tundra: A multi-scale analysis of land cover and evapotranspiration in the Lena River Delta, Siberia, *Tellus, Ser. B*, *64*, doi:10.3402/tellusb.v64i0.17301.

Nicolsky, D., V. Romanovsky, V. Alexeev, and D. Lawrence (2007), Improved modeling of permafrost dynamics in a GCM land-surface scheme, *Geophys. Res. Lett.*, *34*, L08501, doi:10.1029/2007GL029525.

Nicolsky, D., V. Romanovsky, and G. Panteleev (2009), Estimation of soil thermal properties using in-situ temperature measurements in the active layer and permafrost, *Cold Reg. Sci. Technol.*, *55*(1), 120–129, doi:10.1016/j.coldregions.2008.03.003.

O'Donnell, J. A., V. E. Romanovsky, J. W. Harden, and A. D. McGuire (2009), The effect of moisture content on the thermal conductivity of moss and organic soil horizons from black spruce ecosystems in interior Alaska, *Soil Sci.*, *174*(12), 646–651, doi:10.1097/SS.0b013e3181c4a7f8.

Oelke, C., T. Zhang, and M. C. Serreze (2004), Modeling evidence for recent warming of the Arctic soil thermal regime, *Geophys. Res. Lett.*, *31*, L07208, doi:10.1029/2003GL019300.

Osterkamp, T. (2005), The recent warming of permafrost in Alaska, *Global Planet. Change*, *49*(3), 187–202, doi:10.1016/j.gloplacha.2005.09.001.

Painter, S. L. (2011), Three-phase numerical model of water migration in partially frozen geological media: Model formulation, validation, and applications, *Comput. Geosci.*, *15*(1), 69–85, doi:10.1007/s10596-010-9197-z.

Painter, S. L., and S. Karra (2014), Constitutive model for unfrozen water content in subfreezing unsaturated soils, *Vadose Zone J.*, *13*(4), doi:10.2136/vzj2013.04.0071.

Painter, S. L., J. D. Moulton, and C. J. Wilson (2013), Modeling challenges for predicting hydrologic response to degrading permafrost, *Hydrogeol. J.*, *21*(1), 221–224.

Peters-Lidard, C., E. Blackburn, X. Liang, and E. Wood (1998), The effect of soil thermal conductivity parameterization on surface energy fluxes and temperatures, *J. Atmos. Sci.*, *55*(7), 1209–1224, doi:10.1175/1520-0469(1998)055%3C1209:TEOSTC%3E2.0.CO;2.

Rawlins, M., D. Nicolsky, K. McDonald, and V. Romanovsky (2013), Simulating soil freeze/thaw dynamics with an improved pan-Arctic water balance model, *J. Adv. Model. Earth Syst.*, *5*(4), 659–675, doi:10.1002/jame.20045.

Rinke, A., P. Kuhry, and K. Dethloff (2008), Importance of a soil organic layer for Arctic climate: A sensitivity study with an Arctic RCM, *Geophys. Res. Lett.*, *35*, L13709, doi:10.1029/2008GL034052.

Rovansek, R. J., L. D. Hinzman, and D. L. Kane (1996), Hydrology of a tundra wetland complex on the Alaskan arctic coastal plain, USA, *Arct. Alp. Res.*, *28*(3), 311–317, doi:10.2307/1552110.

Rowland, J., B. Travis, and C. Wilson (2011), The role of advective heat transport in talik development beneath lakes and ponds in discontinuous permafrost, *Geophys. Res. Lett.*, *38*, L17504, doi:10.1029/2011GL048497.

Schaefer, K., T. Zhang, A. G. Slater, L. Lu, A. Etringer, and I. Baker (2009), Improving simulated soil temperatures and soil freeze/thaw at high-latitude regions in the Simple Biosphere/Carnegie-Ames-Stanford Approach model, *J. Geophys. Res.*, *114*, F02021, doi:10.1029/2008JF001125.

Schuur, E. A., J. Bockheim, J. G. Canadell, E. Euskirchen, C. B. Field, S. V. Goryachkin, S. Hagemann, P. Kuhry, P. M. Lafleur, and H. Lee (2008), Vulnerability of permafrost carbon to climate change: Implications for the global carbon cycle, *BioScience*, *58*(8), 701–714, doi:10.1641/B580807.

Shur, Y., and M. Jorgenson (2007), Patterns of permafrost formation and degradation in relation to climate and ecosystems, *Permafrost Periglacial Processes*, *18*(1), 7–19, doi:10.1002/ppp.582.

Slater, A. G., and D. M. Lawrence (2013), Diagnosing present and future permafrost from climate models, *J. Clim.*, *26*(15), 5608–5623, doi:10.1175/JCLI-D-12-00341.1.

Sloan, V., J. Liebig, M. Hahn, J. Curtis, J. Brooks, A. Rogers, C. Iversen, and R. Norby (2014), Soil temperature, soil moisture and thaw depth, Barrow, Alaska, Ver. 1*Rep.*, Next Generation Ecosystems Experiment-Arctic, Oak Ridge National Laboratory (ORNL), Oak Ridge, Tenn., doi:10.5440/1121134.

Sturm, M., and J. Holmgren (1994), Effects of microtopography on texture, temperature and heat flow in Arctic and sub-Arctic snow, *Ann. Glaciol.*, *19*, 63–68.

Tarnocai, C., J. Canadell, E. Schuur, P. Kuhry, G. Mazhitova, and S. Zimov (2009), Soil organic carbon pools in the northern circumpolar permafrost region, *Global Biogeochem. Cycles*, *23*, GB2023, doi:10.1029/2008GB003327.

Wainwright, H. M., B. Dafflon, L. J. Smith, M. S. Hahn, J. B. Curtis, Y. Wu, C. Ulrich, J. E. Peterson, M. S. Torn, and S. S. Hubbard (2015), Identifying multiscale zonation and assessing the relative importance of polygon geomorphology on carbon fluxes in an Arctic tundra ecosystem, *J. Geophys. Res. Biogeosci.*, *120*, 788–808, doi:10.1002/2014JG002799.

Westermann, S., M. Langer, J. Boike, M. Heikenfeld, M. Peter, B. Etzelmüller, and G. Krinner (2016), Simulating the thermal regime and thaw processes of ice-rich permafrost ground with the land-surface model CryoGrid 3, *Geosci. Model Dev.*, *9*, 523–546, doi:10.5194/gmd-9-523-2016.

Woo, M.-K., K. L. Young, and L. Brown (2006), High Arctic patchy wetlands: Hydrologic variability and their sustainability, *Phys. Geogr.*, *27*(4), 297–307, doi:10.2747/0272-3646.27.4.297.

Yi, S., M. K. Woo, and M. A. Arain (2007), Impacts of peat and vegetation on permafrost degradation under climate warming, *Geophys. Res. Lett.*, *34*, L16504, doi:10.1029/2007GL030550.

Yi, S., K. Manies, J. Harden, and A. D. McGuire (2009), Characteristics of organic soil in black spruce forests: Implications for the application of land surface and ecosystem models in cold regions, *Geophys. Res. Lett.*, *36*, L05501, doi:10.1029/2008GL037014.

Yi, S., K. Wischnewski, M. Langer, S. Muster, and J. Boike (2014), Freeze/thaw processes in complex permafrost landscapes of northern Siberia simulated using the TEM ecosystem model: Impact of thermokarst ponds and lakes, *Geosci. Model Dev.*, *7*(4), 1671–689, doi:10.5194/gmd-7-1671-2014.

Zhang, T. (2005), Influence of the seasonal snow cover on the ground thermal regime: An overview, *Rev. Geophys.*, *43*, RG4002, doi:10.1029/2004RG000157.

Zona, D., D. Lipson, R. Zulueta, S. Oberbauer, and W. Oechel (2011), Microtopographic controls on ecosystem functioning in the Arctic Coastal Plain, *J. Geophys. Res.*, *116*, G00I08, doi:10.1029/2009JG001241.